Biomaterials 32 (2011) 3115–3123

Contents lists available at ScienceDirect

Biomaterials

journal homepage: www.elsevier.com/locate/biomaterials

Anti-Flt1 peptide – Hyaluronate conjugate for the treatment of retinal neovascularization and diabetic retinopathy

Eun Ju Oh [a,1], Jun-Sub Choi [b,1], Hyemin Kim [a], Choun-Ki Joo [b,**], Sei Kwang Hahn [a,*]

[a] Department of Materials Science and Engineering, Pohang University of Science and Technology (POSTECH), San 31, Hyoja-dong, Nam-gu, Pohang, Kyungbuk 790-784, Republic of Korea

[b] Department of Ophthalmology and Visual Science, Seoul St. Mary's Hospital, College of Medicine, The Catholic University of Korea, 505, Banpo-dong, Seocho-gu, Seoul 137-040, Republic of Korea

ARTICLE INFO

Article history:
Received 18 December 2010
Accepted 4 January 2011
Available online 28 January 2011

Keywords:
Hyaluronate
Anti-Flt1 peptide
Drug delivery
Choroidal neovascularization
Diabetic retinopathy

ABSTRACT

Anti-angiogenic therapeutics has been investigated extensively for the treatment of retinal and choroidal vascular diseases, and diabetic retinopathy. Anti-Flt1 peptide of GNQWFI is an antagonistic peptide for vascular endothelial growth factor receptor 1 (VEGFR1 or Flt1) inhibiting VEGFR1-mediated endothelial cell migration and tube formation. In this work, anti-Flt1 peptide (GGNQWFI) was chemically conjugated to tetra-n-butyl ammonium modified hyaluronate (HA-TBA) via amide bond formation in dimethyl sulfoxide (DMSO) using benzotriazol-1-yloxy-tris(dimethylamino)phosphonium hexafluorophosphate (BOP). The resulting HA – GGNQWFI conjugate self-assembled to form micelle-like nanoparticles in aqueous solution, as confirmed and characterized by transmission electron microscopy (TEM). According to *in vitro* biological activity tests, HA – GGNQWFI conjugate exhibited a dose-dependent inhibition effect on the binding of Flt1-Fc to $VEGF_{165}$ coated on the well. Furthermore, anti-Flt1 peptide – HA conjugate effectively inhibited retinal choroidal neovascularization (CNV) in laser induced CNV model rats. The retinal vascular permeability and the deformation of retinal vascular structure were also significantly reduced in diabetic retinopathy model rats after treatment with anti-Flt1 peptide – HA conjugate. Pharmacokinetic analysis confirmed the increased mean residence time of anti-Flt1 peptide after conjugation to HA longer than 2 weeks.

1. Introduction

Retinal neovascularization is a major cause of retinal vascular leakage, which can induce distortion and loss of central vision in patients with retinal diseases. Among them, age-related macular degeneration (AMD) and diabetic retinopathy (DR) are leading causes of blindness all over the world [1–3]. There are two forms of AMD, dry and wet AMD. Especially, the wet form AMD causes a rapid vision loss and can lead to blindness. Abnormal and fragile blood vessels proliferate in the choroid, which is known as choroidal neovascularization (CNV). The new choroidal vessels leak fluid or blood into the underlying retina causing a significant damage to the retina [2]. Like AMD, DR is also caused by the formation of abnormal blood vessels on the retinal surface [3]. The new fragile blood vessels may leak and bleed into the retina. Under normal conditions, the proliferation of retinal endothelial cells is controlled by the balance between pro-angiogenic factor like vascular endothelial growth factor (VEGF) and anti-angiogenic factor like pigment epithelium derived factor (PEDF) [4]. In both cases of AMD and DR, the expression of VEGF is elevated in the retina leading to angiogenesis and hyperpermeability [5]. Accordingly, the inhibition of VEGF expression and the binding of VEGF to its receptors have been considered as an effective strategy to treat retinal and choroidal vascular diseases, and diabetic retinopathy. Among several anti-angiogenic therapeutics, Ranibizumab (Lucentis®) and Pegaptanib (Macugen®) have been approved by the FDA for the treatment of AMD and are currently in clinical trials for diabetic macular edema (DME) [6,7]. In addition, Bevacizumab (Avastin®) is being widely used off-label for the treatment of AMD and diabetic retinopathy [8]. Anti-Flt1 peptide is an antagonistic peptide for VEGFR1 (fms-like tyrosine kinase-1 or Flt1) that specifically binds to VEGFR1 inhibiting the interaction of VEGFR1 with a variety of VEGFR1 ligands, such as VEGFA, VEGFB, and placental growth factor (PlGF) [9]. Unlike other monoclonal antibodies or RNA antagonists for VEGFR1, anti-Flt1 peptide is a non-immunogenic hexa-peptide which can be easily

* Corresponding author. Tel.: +82 54 279 2159; fax: +82 54 279 2399.
** Corresponding author. Tel.: +82 2 590 2615; fax: +82 2 533 3801.
E-mail addresses: ckjoo@cmc.cuk.ac.kr (C.-K. Joo), skhanb@postech.ac.kr (S.K. Hahn).
[1] These authors contributed equally to this work.

0142-9612/$ – see front matter © 2011 Elsevier Ltd. All rights reserved.
doi:10.1016/j.biomaterials.2011.01.003

synthesized at a low production cost [10]. We previously reported the successful bioconjugation of anti-Flt1 peptide with a sequence of GNQWFI to hyaluronate (HA) [11].

HA is one of the two main structural components of the vitreous in the eye along with collagen [12,13]. HA was first discovered in bovine vitreous humor in 1934 [14]. In addition to the well-known versatile properties of HA, such as biocompatibility, biodegradability, non-immunogenicity, and non-toxicity, recent studies have shown that HA also plays important biological roles in the regulation of vascular endothelial cell migration [15], proliferation [16], and tube formation [17] depending on its molecular weight. HA has a wide molecular weight range from 1000 to 10,000,000 Da. The native high molecular weight HA in tissues degrades into small molecules during the metabolic pathways through lymphatic system, lymph node, liver, and kidney [18]. There are several kinds of HA receptors, such as CD44, LYVE-1, and HARE [19,20]. While the half-life of HA is known to be *ca*. 2.5–5.5 min in plasma [21], it was reported to be *ca*. 70 d in the vitreous body of eyes [22]. The unique physicochemical properties and various biological functions of HA have led to its wide biomedical applications such as drug delivery [23,24], arthritis treatment [25], ocular surgery [26], and tissue engineering [27]. In particular, HA has been investigated extensively for target-specific and long-term delivery of bio/pharmaceuticals through various delivery routes [23]. Taking advantage of its viscoelastic and mucoadhesive properties, HA has been exploited as an effective delivery carrier of topical ophthalmic drugs [28]. A number of studies have reported that HA extended the ocular residence time of ophthalmic drugs [29–31]. In addition, the intraocular injection of HA hydrogel encapsulating gentamicin resulted in the increased half-life in vitrectomized eyes exhibiting an enhanced therapeutic effect on endophthalmitis [32].

In this work, anti-Flt1 peptide – HA conjugates were synthesized and prepared in the form of micelle-like nanoparticles, which were applied as anti-angiogenic therapeutics to the treatment of retinal neovascularization and diabetic retinopathy. After the introduction of glycine to the end of peptide sequence, anti-Flt1 peptide (GGNQWFI) was conjugated to HA-TBA in anhydrous dimethyl sulfoxide (DMSO) using benzotriazol-1-yloxy-tris(dimethylamino)phosphonium hexafluorophosphate (BOP) chemistry. The resulting HA – GGNQWFI conjugate self-assembled to form micelles in aqueous solution, which was confirmed and characterized by transmission electron microscopy (TEM). *In vitro* dose-dependent biological activity of HA – GGNQWFI conjugate was assessed by measuring inhibition effect on the binding of Flt1-Fc to $VEGF_{165}$ coated on the well. With pharmacokinetic analysis, anti-angiogenic effect of HA – GGNQWFI conjugate on retinal choroidal neovascularization (CNV) and diabetic retinopathy was assessed in the laser induced CNV model rats and experimental diabetic rats, respectively.

2. Materials and methods

2.1. Materials

Sodium hyaluronate (HA) with a molecular weight of 100 kDa was obtained from Shiseido Co. (Tokyo, Japan). Anti-Flt1 peptide with a sequence of Gly-Gly-Asn-Gln-Trp-Phe-Ile (GGNQWFI) was purchased from Peptron Co. (Daejeon, Korea). Dowex® 50WX8-40 ion-exchange resin, benzotriazol-1-yloxy-tris(dimethylamino) phosphonium hexafluorophosphate (BOP), N,N-diisopropyl ethylamine (DIPEA), and streptozotocin were purchased from Sigma–Aldrich (St. Louis, MO). Tetra-n-butyl ammonium hydroxide (TBA-OH) was obtained from Alfa Aesar (Ward Hill, MA) and dimethyl sulfoxide (DMSO) from Junsei Chemical Co. (Tokyo, Japan). Human recombinant $VEGF_{165}$ was produced in *Escherichia coli* and purified as described elsewhere [33]. Flt1-Fc was purchased from R&D systems (Minneapolis, MN). Rabbit anti-human IgG-HRP-Fc was obtained from Pierce (Rockford, IL) and BM chemiluminescence ELISA substrate (POD) from Roche (Mannheim, Germany). Ketamine hydrochloride and xylazine hydrochloride were obtained from Yuhan Co. (Seoul, Korea), and Superscript III from Invitrogen (Carlsbad. CA). Epon mixture was obtained from Polyscience (Warrington, PA). All chemicals were used without further purification.

2.2. Preparation of HA-TBA

HA-TBA was prepared as reported elsewhere [11]. Briefly, ion-exchange resin of Dowex® 50WX8-400 (12.5 g) was washed with 250 mL of water three times. Then, 1.5 M excess of TBA-OH (24.5 mL) was added to the Dowex resin and mixed for 30 min. The resulting Dowex-TBA resin was filtered to remove the supernatant. Sodium salt of HA (MW = 100 kDa, 1 g) was dissolved in 100 mL of water, which was poured to the prepared Dowex-TBA resin (10 g). After mixing for 3 h, the supernatant was filtered through 0.45 μm filter to remove the Dowex resin and get a clear HA-TBA solution, and lyophilized for 3 d.

2.3. Synthesis of anti-Flt1 peptide – HA conjugate

Anti-Flt1 peptide (GGNQWFI) and HA-TBA were dissolved in DMSO, respectively. After complete dissolution, HA-TBA was activated by the addition of 2.5 M excess of BOP and mixing for 30 min [11]. Then, the HA-TBA solution was mixed with the peptide and equimolar amount of DIPEA dissolved in DMSO. After reaction at 37 °C for a day, 1 M NaCl aqueous solution was added at a volume ratio of 1/1. The reaction was stopped by dropping the pH of the solution to 3.0 with 1 M HCl and then raising to 7.0 with 1 M NaOH. The resulting product was poured into the pre-washed dialysis membrane tube (MWCO of 10 kDa), dialyzed against a large excess amount of 0.3 M NaCl solution, 25% ethanol, and water, and lyophilized for three days. The peptide content in anti-Flt1 peptide – HA conjugate was determined by fluorometric analysis with a spectrofluorometer (Cary Eclipse Fluorescence Spectrophotometer, Varian, Australia). For the following experiments, anti-Flt1 peptide – HA conjugates with two different peptide contents were used. HA – GGNQWFI (1) conjugate contained 20 peptide molecules per single HA chain and HA – GGNQWFI (2) conjugate contained 28 peptide molecules per single HA chain.

2.4. Characterization of anti-Flt1 peptide – HA conjugate micelles

Anti-Flt1 peptide (GGNQWFI) and HA – GGNQWFI (1) conjugate in a dry powder state were solubilized in 400 μL of PBS to prepare solutions at a final peptide concentration of 1.25 mg/mL. The amount of anti-Flt1 peptide in each solution was measured using changeable UV transilluminator (DUT-260, Core Bio System, Korea). The formation of anti-Flt1 peptide – HA conjugate micelles in aqueous solution was confirmed and visualized by transmission electron microscopy (TEM, Hitachi, Tokyo, Japan). For the TEM analysis, 10 μL drop of HA – GGNQWFI (1) conjugate solution was placed on 300 mesh copper TEM grids with a carbon film and then air-dried. The average particle size was determined from the diameter of 30 particle images.

2.5. In vitro biological activity tests of anti-Flt1 peptide – HA conjugate

$VEGF_{165}$ solution at a concentration of 0.5 μg/mL in PBS was incubated in 96-black well-plate at 4 °C overnight for the preparation of $VEGF_{165}$ coated wells. After washing with PBS, the wells were blocked with a blocking buffer of 3 wt% bovine serum albumin (BSA) in PBS at room temperature for 2 h and washed with PBS again. Anti-Flt1 peptide (GGNQWFI) or HA – GGNQWFI (1) conjugate solution containing 20–20,000 nM of peptide and 500 ng/mL of Flt1-Fc in 1 wt% BSA solution in PBS was added to the well and incubated at room temperature for 1 h. The solution containing 500 ng/mL of Flt1-Fc in 1 wt% BSA solution in PBS without peptide was used as a positive control. After washing thrice with PBS containing 0.05 wt% of Tween 20, anti-human IgG-HRP-Fc in 0.3 wt% BSA solution in PBS was added and incubated at room temperature for 1 h. Finally, after washing thrice with PBS containing 0.05% of Tween 20 and once with PBS, the amount of bound Flt1-Fc was measured with a BM chemiluminescence ELISA substrate system (Victor 3 luminometer, Perkin Elmer, MA). ELISA was performed twice with three replicates.

2.6. Retinal choroidal anti-neovascularization tests

The retinal choroidal anti-neovascularization test was carried out using four groups of Brown-Norway (BN) male rats at an age of 8 weeks with a mean body weight of 250 g: Group 1 – Negative control group where CNV was induced and untreated during the test; Group 2 – HA treated group where CNV was induced and treated with HA; Group 3 – Peptide treated group where CNV was induced and treated with anti-Flt1 peptide (GGNQWFI) (10 mg/mL); Group 4 – Conjugate (2) treated group where CNV was induced and treated with HA – GGNQWFI (2) conjugate. The injection vehicle was PBS. For comparison, the peptide content in HA – GGNQWFI (2) conjugate sample was adjusted to be equivalent to that of anti-Flt1 peptide sample at a value of 10 mg/mL. Six retinal choroids were tested and analyzed in each group. Before the tests, BN rats were anesthetized with 0.2 mL of 1/1 mixture of ketamine hydrochloride (100 mg/mL) and xylazine hydrochloride (20 mg/mL). Then, pupils were dilated with a topical application of 0.8% tropicamide. CNV was experimentally induced by intense laser photocoagulation with a wavelength of 532 nm (Visulas 532, Carl Zeiss, Germany) to disrupt the retinal Bruch's membrane

(spot size 100 μm, power 260 mA, exposure time 30 ms). On the third day after laser injury, each 10 μL of the sample solution was intravitreally injected. The inhibitory effect on CNV in the retina was confirmed by fluorescence microscopy using dextran-FITC (MW = 40,000) 2 weeks after laser injury. After anesthesia, 500 μL of dextran-FITC solution (25 mg/mL) was injected into the tail vein of BN rats. Five min later, the retinas were isolated and observed under a fluorescence microscope (Olympus, Tokyo, Japan) with a digital camera. The captured images were analyzed by Image J program (NIH, Bethesda, MD).

2.7. Diabetic retinopathy tests

The inhibitory effect of anti-Flt1 peptide – HA conjugate on vascular hyperpermeability in experimental diabetic retinopathy was assessed using four groups of Sprague Dawley (SD) male rats at an age of 8 weeks with a mean body weight of 250 g: Group 1 – HA treated group where diabetes was induced and treated with HA; Group 2 – Peptide treated group where diabetes was induced and treated with anti-Flt1 peptide (GGNQWFI) (5 mg/mL); Group 3 – Conjugate (1) treated group where diabetes was induced and treated with HA – GGNQWFI (1) conjugate; Group 4 – Conjugate (2) treated group where diabetes was induced and treated with HA – GGNQWFI (2) conjugate. The injection vehicle was PBS. For comparison, the peptide content in anti-Flt1 peptide – HA conjugate samples was adjusted to be equivalent to that of anti-Flt1 peptide sample at a value of 5 mg/mL. Ten retinas were tested and analyzed in each group. Before the tests, diabetes was induced by a single intraperitoneal injection of streptozotocin to SD rats at a dose of 60 mg/kg in 10 mM citrate buffer at pH 4.5. Three days after streptozotocin injection, SD rats with a plasma glucose concentration higher than 300 mg/dL were considered to be diabetic. Each 10 μL of sample solution was injected intravitreally 1 week after streptozotocin injection. The inhibitory effect on vascular hyperpermeability caused by experimental diabetic retinopathy was assessed by fluorescence microscopy using dextran-FITC (MW = 10,000) 4 weeks after streptozotocin injection as described in the Section 2.6. In addition, the change of retinal vascular structure was observed by electron microscopy. Briefly, the retinas were enucleated and fixed in 4 wt% glutaraldehyde and 1 wt% osmium tetroxide solution. The fixed retinas were dehydrated with ethanol and embedded in Epon mixture. Then, the samples were sectioned and observed under a transmission electron microscope (JEM-1010, JEOL, Tokyo, Japan).

2.8. Pharmacokinetic analysis

Pharmacokinetic (PK) analysis of anti-Flt1 peptide – HA conjugate was carried out using three groups of SD rats at an age of 8 weeks with a mean body weight of 250 g: Group 1 – HA injected group; Group 2 – Peptide injected group using anti-Flt1 peptide (GGNQWFI) (5 mg/mL); Group 3 – Conjugate (1) injected group using HA – GGNQWFI (1) conjugate. The injection vehicle was PBS. For comparison, the peptide content in HA – GGNQWFI (1) conjugate sample was adjusted to be equivalent to that of anti-Flt1 peptide sample at a value of 5 mg/mL. Six vitreous bodies were tested and analyzed in each group at each sampling time. After intravitreal injection of each 10 μL of the sample solution, the vitreous bodies were collected in 6 h, 1, 3, 7, 10, and 14 d. The collected vitreous bodies were stored at −20 °C before analysis. The concentration of anti-Flt1 peptide in vitreous body was measured by fluorometric analysis. After lysis of vitreous body with 200 μL of RIPA buffer, the supernatant was obtained by centrifugation at 14,000 g and 4 °C for 10 min. Then, the photo-luminescence of samples was measured with a spectrofluorometer (Cary Eclipse Fluorescence Spectrophotometer, Varian, Australia) with an excitation wavelength of 280 nm and an emission wavelength of 350 nm. The average fluorescence from six vitreous bodies of untreated SD rats was used as a blank control. All animal procedures conformed to the guidelines of the Catholic University of Korea and *the principles of laboratory animal care* (NIH publication No. 85-23 revised in 1985).

2.9. Statistical analysis

The data were expressed as Mean ± S.D. from several separate experiments. Statistical analysis was carried out via *t*-test using a software of Sigma Plot 9.0 and a value for $P < 0.05$ was considered statistically significant.

3. Results and discussion

3.1. Anti-Flt1 peptide – HA conjugate micelles in aqueous solution

Water-insoluble anti-Flt1 peptide (GNQWFI), an effective anti-angiogenic drug, was chemically conjugated to HA in organic solvent for the treatment of retinal neovascularization and diabetic retinopathy. Fig. 1a shows the primary structure of anti-Flt1 peptide. There are two amino acids with a ring structure in anti-Flt1 peptide, tryptophan (W) and phenylalanine (F). They are located close to the C-terminal which is the opposite side of glycine, and their aromatic side chains are relatively nonpolar and hydrophobic. The normalized hydrophobicity indexes (HI) for tryptophan and phenylalanine are 97 and 100 at pH 7, respectively [34]. In addition, isoleucine (I) on the C-terminal is hydrophobic due to its hydrocarbon side chain (HI = 99 at pH 7). In contrast, the two amino acids next to glycine on the N-terminal, asparagine (N, HI = −28 at pH 7) and glutamine (Q, HI = −10 at pH 7), are relatively polar and hydrophilic. Since glycine (G, HI = 0 at pH 7) is neutral in terms of hydrophobicity, the first half of anti-Flt1 peptide sequence from glycine to glutamine near the N-terminal is supposed to be slightly hydrophilic, whereas the remaining half from tryptophan to isoleucine near the C-terminal to be highly hydrophobic. In total, the anti-Flt1 peptide is hydrophobic due to the strong hydrophobic domain with high HI values on its amino acid sequence, which explains its poor solubility in aqueous solution as shown in the photographic image of Fig. 1b. As we previously reported elsewhere [11], the bioconjugation of HA with the peptide was carried out in a single organic phase. To make HA soluble in organic solvent, HA-TBA was prepared in aqueous solution by the ion-exchange method. The freeze-dried HA-TBA was clearly dissolved in anhydrous DMSO. After activation of carboxyl groups of HA with BOP, anti-Flt1 peptide with additional glycine (GGNQWFI) was mixed with HA-TBA to synthesize HA–GGNQWFI conjugate by the formation of amide linkage between carboxyl groups of HA and α-amines at the N-terminal of anti-Flt1 peptide. After conjugation reaction, the solvent was exchanged from DMSO to water by a series of dialysis and then lyophilized. The successful formation of anti-Flt1 peptide – HA conjugate was confirmed by ^{1}H NMR analysis and the peptide content in anti-Flt1 peptide – HA conjugate was determined by measuring the fluorescence intensity of tryptophan. The solubility of anti-Flt1 peptide was significantly enhanced after conjugation to HA. Fig. 1b shows the completely transparent solution of HA – GGNQWFI (1) conjugate under visible light in comparison to the turbid anti-Flt1 peptide solution. Since tryptophan shows fluorescence under UV, the amount of anti-Flt1 peptide in the solution can be determined by measuring the fluorescence intensity. Two samples had the same amount of anti-Flt1 peptide exhibiting equivalent fluorometric intensity from tryptophan under UV (Fig. 1b). In the photograph taken under UV, anti-Flt1 peptide without HA was precipitated in a cluster with increasing time whereas HA – GGNQWFI (1) conjugate was uniformly dispersed resulting in homogeneous solution. The TEM image in Fig. 1c shows the spherical morphology of HA – GGNQWFI (1) conjugate micelles with a mean diameter of 234.5 ± 20.6 nm ($n = 30$). It was thought that anti-Flt1 peptide – HA conjugate self-assembled into micelle-like nanoparticles in aqueous solution by the hydrophobic interaction of anti-Flt1 peptide in the conjugate. The strongly hydrophobic domain of anti-Flt1 peptide might form hydrophobic inner core surrounded by hydrophilic outer-layer of HA. The well-balanced amphiphilic anti-Flt1 peptide might be advantageous for the micelle formation. The relatively hydrophilic domain (GNQ) of anti-Flt1 peptide might facilitate the conjugation reaction with hydrophilic HA molecules and then the highly hydrophobic domain (WFI) of anti-Flt1 peptide might contribute to the micelle formation.

3.2. In vitro biological activity of anti-Flt1 peptide – HA conjugate

In vitro dose-dependent biological activity of anti-Flt1 peptide – HA conjugate was assessed by monitoring the inhibition effect on the binding of Flt1-Fc to $VEGF_{165}$ coated on the well. As a VEGFR1 (Flt1)-specific antagonistic peptide, anti-Flt1 peptide specifically binds to Flt1 and interrupts the interaction of Flt1 with other Flt1 ligands like

$VEGF_{165}$. After treatment of the mixed solution of anti-Flt1 peptide (GGNQWFI) and Flt1-Fc, unbound Flt1-Fc was removed and the remaining Flt1-Fc bound to $VEGF_{165}$ was detected by ELISA. As shown in Fig. 2, the luminescence value for a positive control without anti-Flt1 peptide was set to be 100% and the other data were normalized in comparison to the value. Up to 200 nM, anti-Flt1 peptide did not reduce the binding of Flt1-Fc to $VEGF_{165}$, and even at the higher concentration, *ca.* 68% of $VEGF_{165}$ bound to Flt1-Fc. In contrast, HA – GGNQWFI (1) conjugate effectively reduced the binding of Flt1-Fc to $VEGF_{165}$ down to *ca.* 32% and showed a dose-dependently increasing inhibitory effect within the entire peptide concentration range. The enhanced biological activity of anti-Flt1 peptide after conjugation to HA might be ascribed to the improved solubility in aqueous solution. Unlike water-insoluble anti-Flt1 peptide, anti-Flt1 peptide – HA conjugate was distributed uniformly in the solution readily contacting with Flt1-Fc. The $VEGF_{165}$ binding test by ELISA clearly confirmed the inhibition effect of anti-Flt1 peptide – HA conjugate on the binding of Flt1-Fc to $VEGF_{165}$ in a dose-dependent manner.

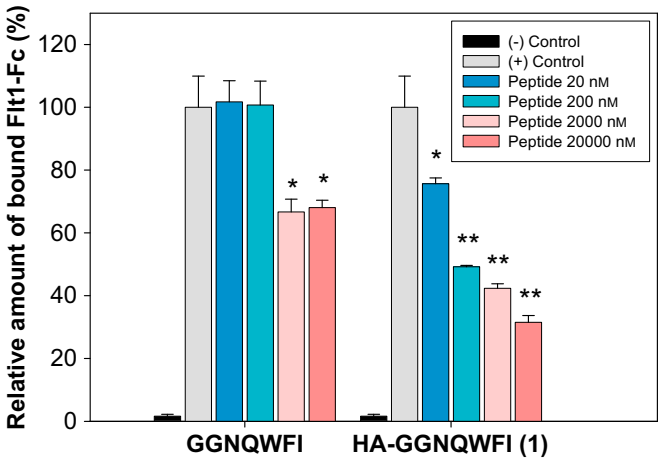

Fig. 2. *In vitro* biological activity of anti-Flt1 peptide (GGNQWFI) and HA–GGNQWFI conjugate inhibiting the binding of Flt1-Fc to VEGF165 coated on the well with increasing peptide concentrations. Data are presented as means ± S.D. $^{*}P < 0.05$ and $^{**}P < 0.01$ versus the positive control group ($n = 3$).

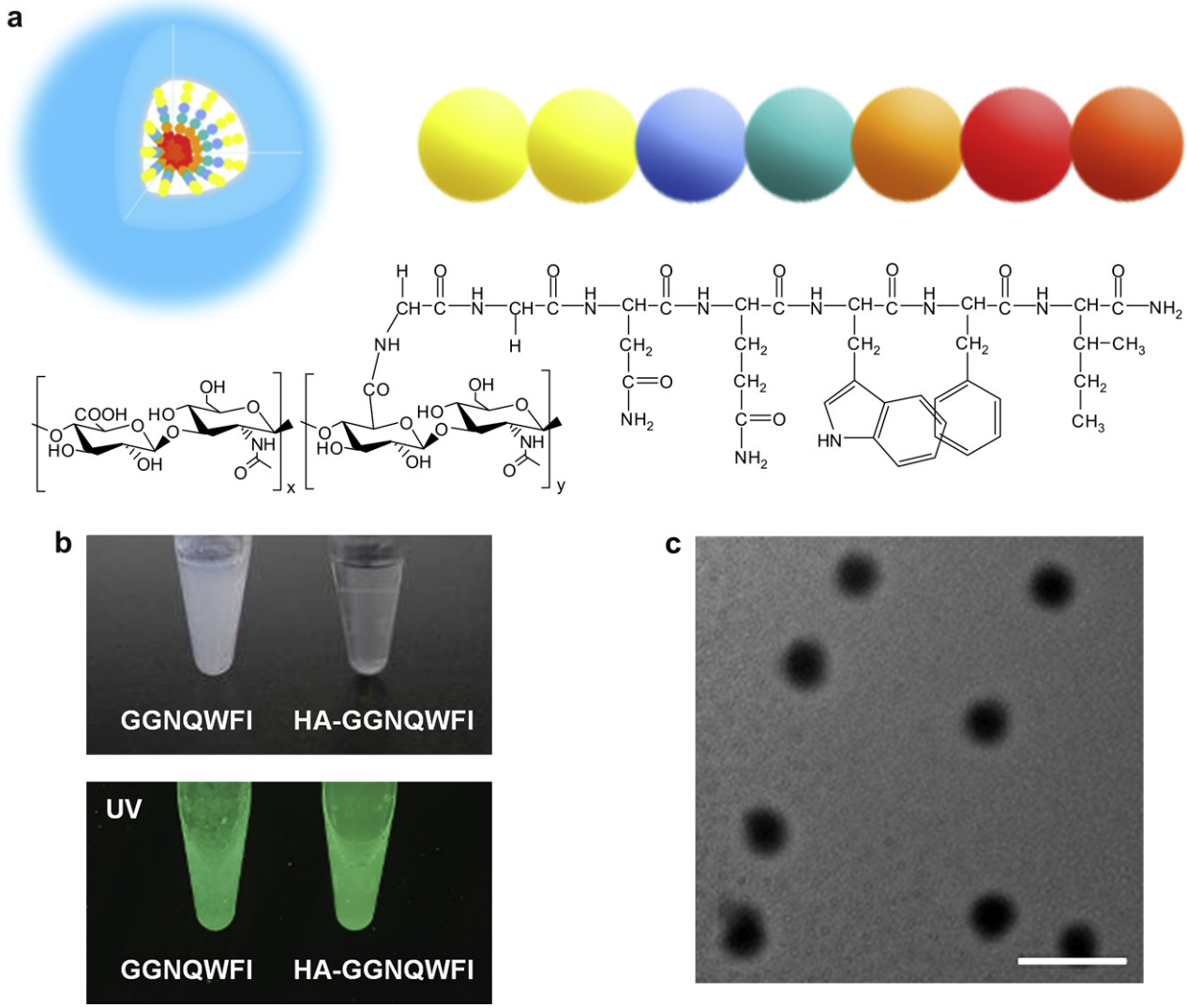

Fig. 1. (a) Schematic representation of HA–anti-Flt1 peptide (GGNQWFI) conjugate micelle and chemical structure of HA–GGNQWFI conjugate. (b) Photographs of anti-Flt1 peptide and HA–GGNQWFI conjugate aqueous solutions under visible light (top) and UV (bottom). (c) Transmission electron microscopic (TEM) image of HA–GGNQWFI conjugate micelles. Scale bar corresponds to 500 nm.

3.3. Inhibitory effect of anti-Flt1 peptide – HA conjugate on choroidal neovascularization

The inhibitory effect of anti-Flt1 peptide – HA conjugate on CNV in the retina was assessed in laser induced CNV model BN rats. Three kinds of samples, HA, anti-Flt1 peptide (GGNQWFI), and HA – GGNQWFI (2) conjugate, were injected into the vitreous of BN rats 3 d after laser injury, and the inhibitory effect was assessed by the analysis of fluorescence microscopic images in 2 weeks. Fig. 3 shows the dextran-FITC fluorescence in the retina demonstrating the inhibitory effect of anti-Flt1 peptide and anti-Flt1 peptide – HA conjugate on CNV. In the negative control and HA treated groups, high fluorescence intensity and large lesion on Burch's membrane were observed, whereas anti-Flt1 peptide and anti-Flt1 peptide – HA conjugate groups showed low fluorescence intensity and small lesion. Anti-Flt1 peptide – HA conjugate resulted in a more effective inhibition of CNV than anti-Flt1 peptide alone. The inhibitory effect in each experimental group was quantified and represented in Fig. 4. The mean fluorescence intensity for a negative control was set to be 100% and the other data were normalized in comparison to the value. The mean percentage of fluorescence intensity was 97.1 ± 4.7% after treatment with HA, 61.4 ± 4.4% after treatment with anti-Flt1 peptide, and 48.9 ± 3.9% after treatment with anti-Flt1 peptide – HA conjugate, respectively. According to the statistical analysis by *t*-test, anti-Flt1 peptide and anti-Flt1 peptide – HA conjugate resulted in the significant decrease of fluorescence intensity compared to the negative control and HA ($^{**}P < 0.01$). Furthermore, the inhibitory effect of anti-Flt1 peptide – HA

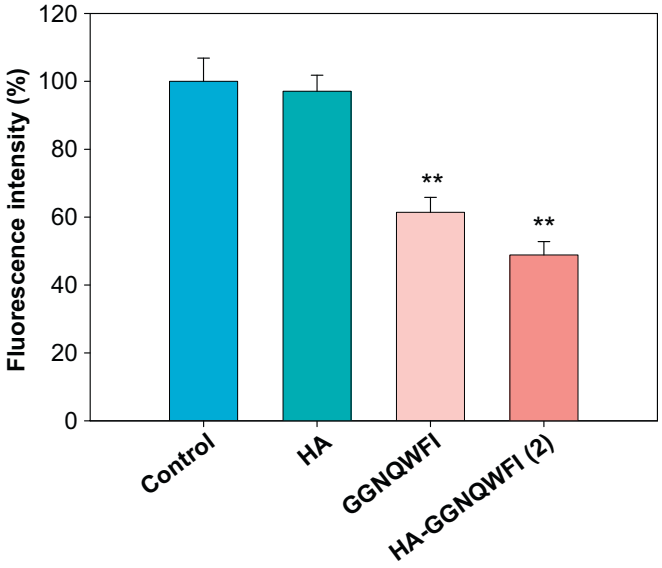

Fig. 4. Fluorescence intensity of retinal choroidal neovascularization lesions in Brown-Norway male rats treated with control, HA, anti-Flt1 peptide (GGNQWFI), and HA–GGNQWFI (2) conjugate 2 weeks after laser induced injury. The fluorescence intensity was quantified by Image J program and represented as means ± S.D. $^{**}P < 0.01$ versus the control group ($n = 6$).

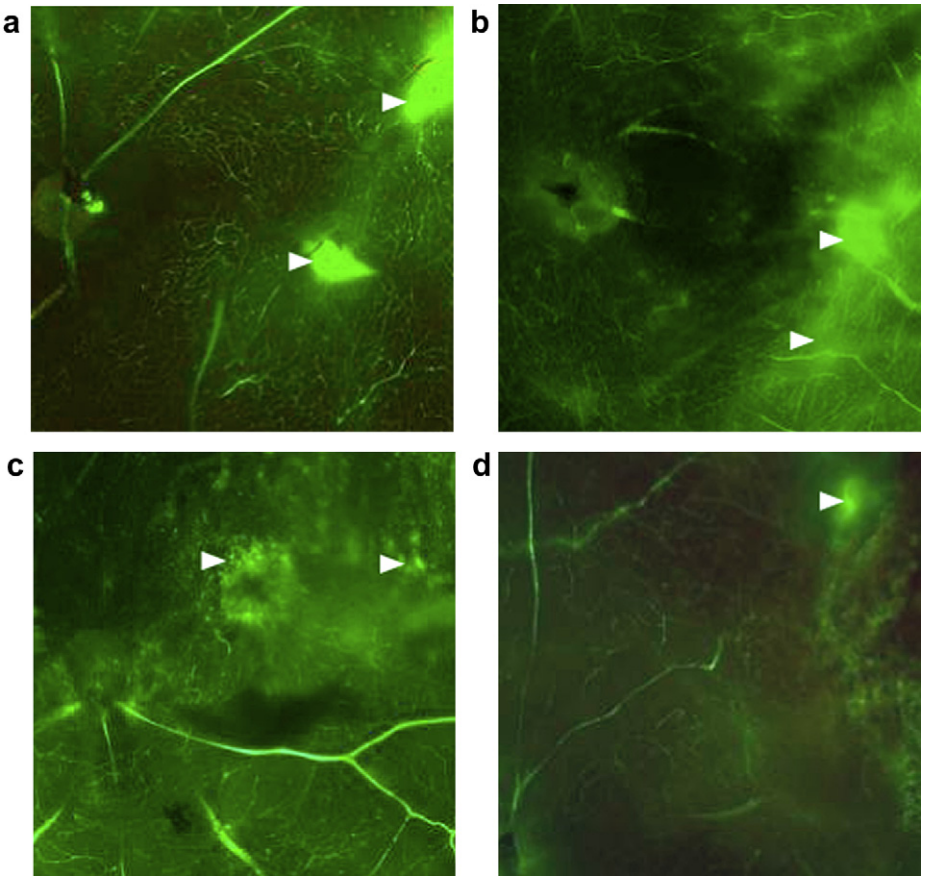

Fig. 3. In vivo inhibitory effect of anti-Flt1 peptide (GGNQWFI) and HA–GGNQWFI conjugate on laser induced retinal choroidal neovascularization: Fluorescence microscopy of the retina in Brown-Norway male rats treated with (a) Control, (b) HA, (c) GGNQWFI, and (d) HA–GGNQWFI (2) conjugate 2 weeks after laser induced injury. Original magnification was ×100.

conjugate was obviously more significant than anti-Flt1 peptide ($P = 0.0004$).

3.4. Inhibitory effect of anti-Flt1 peptide – HA conjugate on diabetic retinopathy

In order to assess the inhibitory effect of anti-Flt1 peptide – HA conjugate on diabetic retinal vascular permeability, four kinds of samples, HA, anti-Flt1 peptide (GGNQWFI), HA – GGNQWFI (1) conjugate, and HA – GGNQWFI (2) conjugate, were injected into the vitreous of SD rats 1 week after streptozotocin injection. The inhibitory effect was evaluated by fluorescence microscopic and electron microscopic analyses after injection of dextran-FITC in 4 weeks. Fig. 5 shows the dextran-FITC fluorescence in the retina demonstrating the inhibitory effect of anti-Flt1 peptide and anti-Flt1 peptide – HA conjugate on retinal vascular hyperpermeability in the experimental diabetic retinopathy. For the case of HA treated group, the fluorescence of dextran-FITC was shown throughout the retinal parenchyma due to the increased vascular leakage after blood retinal barrier (BRB) breakdown. In the anti-Flt1 peptide and anti-Flt1 peptide – HA conjugate groups, little fluorescence was shown in the retinal parenchyma and dextran-FITC fluorescence was observed in the vasculature revealing the retinal vessels. Anti-Flt1 peptide – HA conjugates resulted in more significant decrease in the level of retinal vascular permeability than anti-Flt1 peptide alone. The inhibitory effect in each experimental group was quantified and represented in Fig. 6. The mean fluorescence intensity for the HA group was set to be 100% and the other data were normalized. The mean percentage of fluorescence intensity was 79.0 ± 9.2% after treatment with anti-Flt1 peptide, 58.4 ± 7.8% after treatment with HA – GGNQWFI (1) conjugate, and 51.3 ± 10.8% after treatment with HA – GGNQWFI (2) conjugate, respectively. According to the statistical analysis by *t*-test, anti-Flt1 peptide and anti-Flt1 peptide – HA conjugate resulted in a more significant decrease of fluorescence intensity than HA (**$P < 0.01$), and the inhibitory effect of anti-Flt1 peptide – HA conjugates was more significant than anti-Flt1 peptide alone ($P < 0.01$). In addition, HA – GGNQWFI (2) conjugate with a higher peptide content reduced fluorescence intensity more

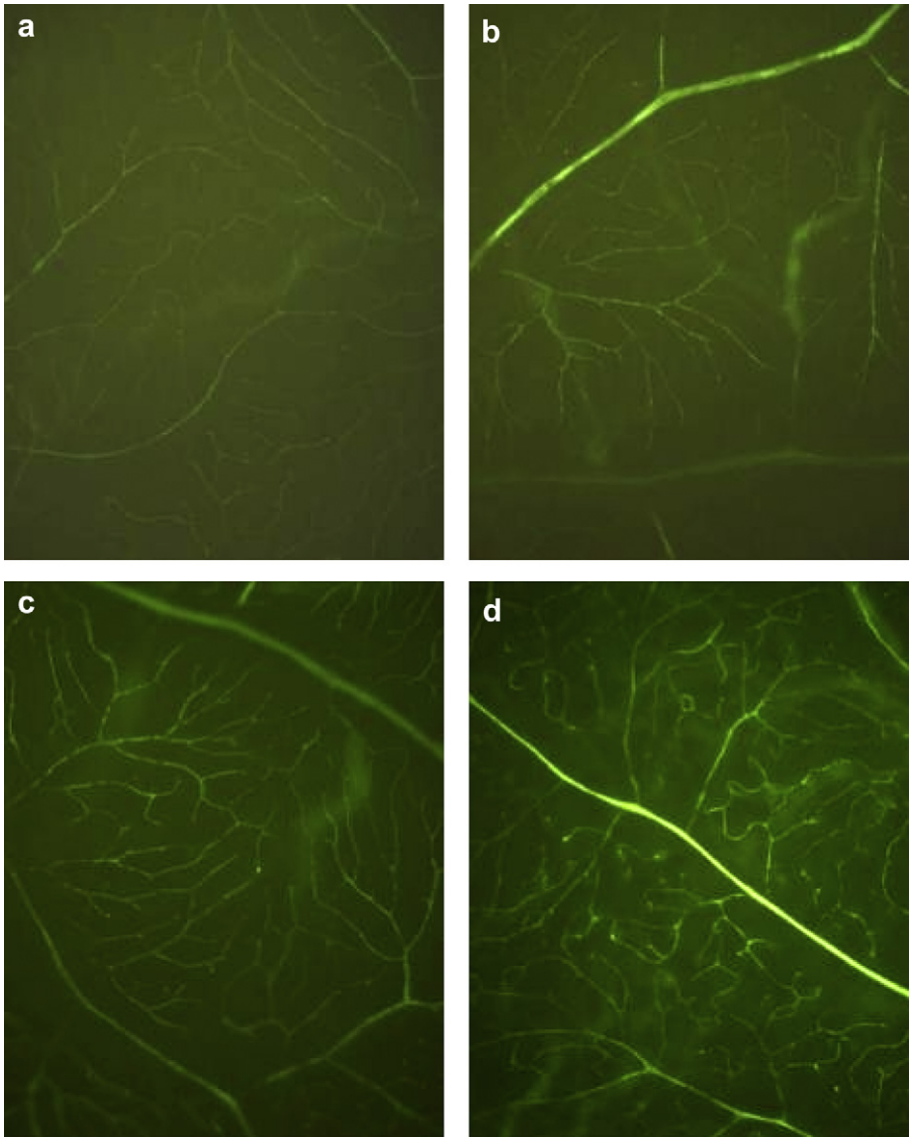

Fig. 5. In vivo inhibitory effect of anti-Flt1 peptide (GGNQWFI) and HA–GGNQWFI conjugate on the vascular hyperpermeability by streptozotocin induced diabetic retinopathy: Fluorescence microscopy of the retina in SD rats treated with (a) HA, (b) GGNQWFI, (c) HA–GGNQWFI (1) conjugate, and (d) HA–GGNQWFI (2) conjugate 4 weeks after streptozotocin injection. Original magnification was ×100.

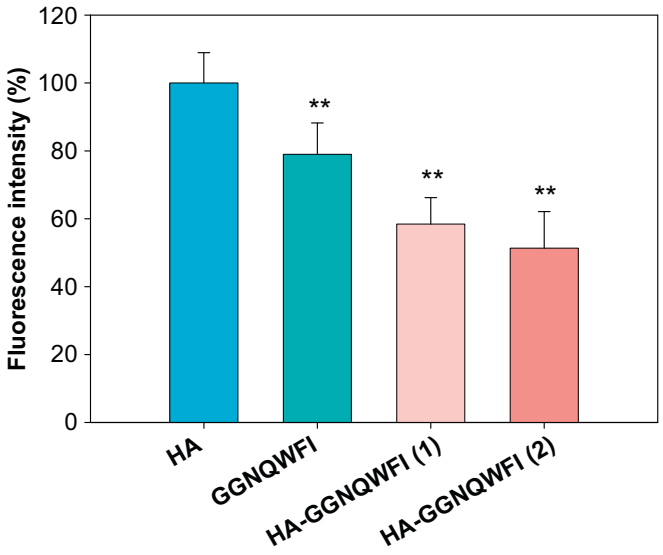

Fig. 6. Fluorescence intensity of the retina in SD rats treated with HA, anti-Flt1 peptide (GGNQWFI), HA–GGNQWFI (1) conjugate, and HA–GGNQWFI (2) conjugate 4 weeks after streptozotocin injection. The fluorescence intensity was quantified by Image J program and represented as means ± S.D. $^{**}P < 0.01$ versus the control group of HA treatment ($n = 10$).

effectively than HA – GGNQWFI (1) conjugate ($P = 0.1$). The therapeutic effect was also assessed by the electron microscopic analysis of the morphological change of the retinal vascular structure. In the diabetic retina, the vascular basement membrane had an irregular and folded shape with a thin vascular endothelial cell layer reflecting the increased vascular permeability (Fig. 7b). The diabetic retinal vessel after treatment with anti-Flt1 peptide had a round shape, although the surrounding vascular endothelial cell layer was not as thick as that of the normal retinal vessel (Fig. 7c). In contrast, the diabetic retinal vessel after treatment with anti-Flt1 peptide – HA conjugate had a round shape surrounded by a thick vascular endothelial cell layer (Fig. 7d), which was comparable to the structure of a normal retinal vessel (Fig. 7a). The electron microscopic analysis clearly visualized the enhanced inhibition effect of anti-Flt1 peptide after conjugation to HA on the deformation of retinal vascular structure in diabetic SD rats.

3.5. Pharmacokinetic analysis of anti-Flt1 peptide – HA conjugate

Pharmacokinetic analysis of anti-Flt1 peptide – HA conjugate was carried out in SD rats after a single intravitreal injection of three kinds of samples, HA, anti-Flt1 peptide (GGNQWFI), and HA – GGNQWFI (1) conjugate. The dose of HA and anti-Flt1 peptide was separately adjusted to be equivalent to each dose in HA – GGNQWFI (1) conjugate group. As tryptophan in anti-Flt1 peptide showed a sharp emission peak at 350 nm after excitation at a wavelength of 280 nm, the concentration of anti-Flt1 peptide in the vitreous body could be determined by measuring the fluorescence intensity of tryptophan in

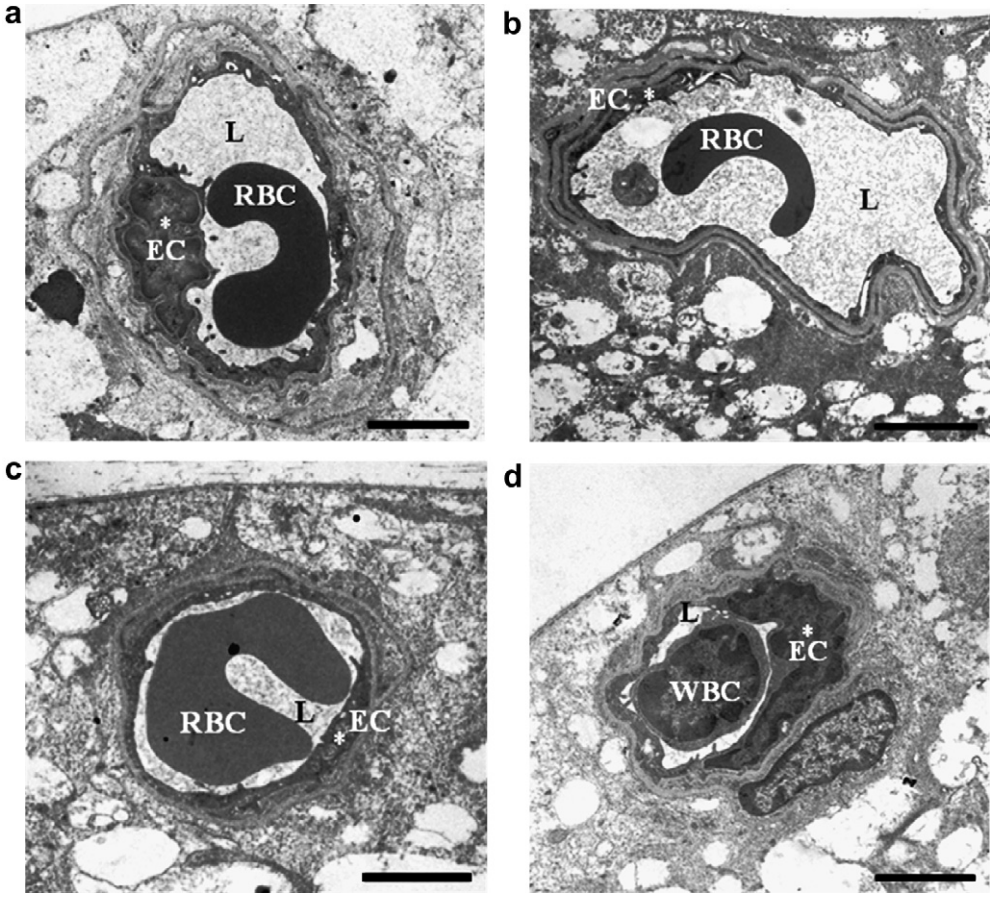

Fig. 7. Electron micrographs of the retinal vessels in SD rats: (a) Normal control without diabetic retinopathy, (b) Negative control with streptozotocin induced diabetic retinopathy, (c) Anti-Flt1 peptide (GGNQWFI) treated diabetic retina, and (d) HA–GGNQWFI (2) conjugate treated diabetic retina (L: lumen of vessel, *EC: endothelial cell, RBC: red blood cell, WBC: white blood cell). Scale bar corresponds to 2 μm.

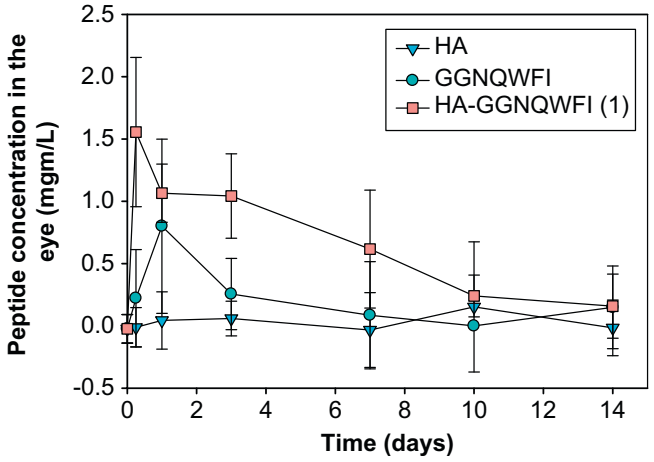

Fig. 8. Pharmacokinetics of anti-Flt1 peptide in the vitreous bodies of Sprague Dawley rats after an intravitreal single injection of sample solutions containing HA, anti-Flt1 peptide (GGNQWFI), and HA–GGNQWFI conjugate. Data are represented as means ± S.D. ($n = 6$).

the vitreous humor. After a single administration, the elevated intravitreal concentration of anti-Flt1 peptide – HA conjugate maintained for longer than 14 days with a T_{max} of 6 h, whereas the intravitreal concentration of anti-Flt1 peptide dropped to the baseline level within 7 d with a T_{max} of 24 h (Fig. 8). The relatively long T_{max} in anti-Flt1 peptide group might be attributed to the slow dissolution of poorly soluble anti-Flt1 peptide dispersed in PBS. The C_{max} of intravitreal concentration resulted from anti-Flt1 peptide – HA conjugate was 1.6 ± 0.6 mg/mL, which was higher than that of anti-Flt1 peptide (0.8 ± 0.7 mg/mL) with the equivalent peptide dose. The AUC for anti-Flt1 peptide – HA conjugate was also higher than that for anti-Flt1 peptide in spite of the same peptide dose, indicating the increased bioavailability (AUC/dose) of anti-Flt1 peptide after conjugation to HA. The bioconjugation of anti-Flt1 peptide to HA effectively prevented the clearance of anti-Flt1 peptide by reducing both the escape of anti-Flt1 peptide from the vitreous body to other tissues and the enzymatic degradation of anti-Flt1 peptide in the vitreous humor. Taken together, anti-Flt1 peptide – HA conjugate was thought to be successfully developed for the treatment of retinal choroidal neovascularization and vascular hyperpermeability in diabetic retinopathy. The improved water-solubility and bioavailability of anti-Flt1 peptide after conjugation to HA might be advantageous for further clinical applications. Moreover, anti-Flt1 peptide – HA conjugate having a micelle structure in aqueous solution can be successfully exploited as a novel drug carrier of various hydrophobic drugs with its own anti-angiogenic effect.

4. Conclusions

Anti-Flt1 peptide, a water-insoluble anti-angiogenic peptide drug, was successfully conjugated to HA-TBA by the formation of amide linkage in anhydrous DMSO using BOP as a coupling reagent. The resulting anti-Flt1 peptide – HA conjugates self-assembled to form spherical micelle-like nanoparticles in aqueous solution with an average diameter of 234.5 ± 20.6 nm. According to *in vitro* test, anti-Flt1 peptide – HA conjugate showed a dose-dependent biological activity inhibiting the binding of Flt1-Fc to $VEGF_{165}$ coated on the well, which was more effective than the peptide without conjugation likely due to the improved water-solubility. The inhibitory effect of anti-Flt1 peptide – HA conjugate on the retinal CNV was confirmed in laser induced CNV model BN rats by fluorescence microscopic analysis. In diabetic retinopathy model SD rats, anti-Flt1 peptide – HA conjugate also effectively inhibited the retinal vascular hyperpermeability and the deformation of retinal vascular structure as shown in the fluorescence microscopic and electron microscopic analyses. Pharmacokinetic images revealed the increased stability and bioavailability of anti-Flt1 peptide after conjugation to HA. Taken together, anti-Flt1 peptide – HA conjugate was thought to be successfully developed for the treatment of retinal choroidal neovascularization and diabetic retinopathy. Furthermore, anti-Flt1 peptide – HA conjugate having a nano-size micelle structure in aqueous solution can be successfully exploited as a drug carrier of hydrophobic anti-angiogenic drugs for a cocktail therapy.

Acknowledgment

This study was supported by a grant of the Korea Healthcare Technology R&D Project, Ministry of Health & Welfare, Republic of Korea (A080711). This work was also supported by Mid-career Researcher Program through NRF grant funded by the MEST (No. 2009-0084578).

Appendix

Figures with essential color discrimination. Figs. 1–6 and 8 in this article have parts that are difficult to interpret in black and white. The full color images can be found in the online version, at doi:10.1016/j.biomaterials.2011.01.003

References

[1] Gehrs KM, Anderson DH, Johnson LV, Hageman GS. Age-related macular degeneration - emerging pathogenetic and therapeutic concepts. Ann Med 2006;38:450–71.
[2] Nowak JZ. Age-related macular degeneration (AMD): pathogenesis and therapy. Pharmacol Rep 2006;58:353–63.
[3] Frank RN. Diabetic retinopathy. N Engl J Med 2004;350:48–58.
[4] Armulik A, Abramsson A, Betsholtz C. Endothelial/pericyte interactions. Circ Res 2005;97:512–23.
[5] Hammes HP, Lin J, Bretzel RG, Brownlee M, Breier G. Upregulation of the vascular endothelial growth factor/vascular endothelial growth factor receptor system in experimental background diabetic retinopathy of the rat. Diabetes 1998;47:401–6.
[6] Starita C, Patel M, Katz B, Adamis A. Vascular endothelial growth factor and the potential therapeutic use of pegaptanib (macugen) in diabetic retinopathy. Dev Ophthalmol 2007;39:122–48.
[7] Rodrigues EB, Farah ME, Maia M, Penha FM, Regatieri C, Melo GB, et al. Therapeutic monoclonal antibodies in ophthalmology. Prog Retin Eye Res 2009;28:117–44.
[8] Rosenfeld PJ, Brown DM, Heier JS, Boyer DS, Kaiser PK, Chung CY, et al. Ranibizumab for neovascular age-related macular degeneration. N Engl J Med 2006;355:1419–31.
[9] Bae DG, Kim TD, Li G, Yoon WH, Chae CB. Anti-Flt1 peptide, a vascular endothelial growth factor receptor 1-specific hexapeptide, inhibits tumor growth and metastasis. Clin Cancer Res 2005;11:2651–61.
[10] Luttun A, Tjwa M, Moons L, Wu Y, Angelillo-Scherrer A, Liao F, et al. Revascularization of ischemic tissues by PlGF treatment, and inhibition of tumor angiogenesis, arthritis and atherosclerosis by anti-Flt1. Nat Med 2002;8:831–40.
[11] Oh EJ, Park K, Choi JS, Joo CK, Hahn SK. Synthesis, characterization, and preliminary assessment of anti-Flt1 peptide–hyaluronate conjugate for the treatment of corneal neovascularization. Biomaterials 2009;30:6026–34.
[12] Laurent TC, Fraser JR. Hyaluronan. FASEB J 1992;6:2397–404.
[13] Bishop P. The biochemical structure of mammalian vitreous. Eye 1996;10 (Pt6):664–70.
[14] Meyer K, Palmer JW. The polysaccharide of the vitreous humor. J Biol Chem 1934;107:629–34.
[15] Sattar A, Rooney P, Kumar S, Pye D, West DC, Scott I, et al. Application of angiogenic oligosaccharides of hyaluronan increases blood vessel numbers in rat skin. J Invest Dermatol 1994;103:576–9.
[16] Slevin M, Kumar S, Gaffney J. Angiogenic oligosaccharides of hyaluronan induce multiple signaling pathways affecting vascular endothelial cell mitogenic and wound healing responses. J Biol Chem 2002;277:41046–59.
[17] Montesano R, Kumar S, Orci L, Pepper MS. Synergistic effect of hyaluronan oligosaccharides and vascular endothelial growth factor on angiogenesis *in vitro*. Lab Invest 1996;75:249–62.
[18] Stern R. Hyaluronan catabolism: a new metabolic pathway. Eur J Cell Biol 2004;83:317–25.

[19] Banerji S, Ni J, Wang SX, Clasper S, Su J, Tammi R, et al. LYVE-1, a new homologue of the CD44 glycoprotein, is a lymph-specific receptor for hyaluronan. J Cell Biol 1999;144:789–801.
[20] Zhou B, Weigel JA, Fauss LA, Weigel PH. Identification of the hyaluronan receptor for endocytosis (HARE). J Biol Chem 2000;275:37733–41.
[21] Fraser JRE, Laurent TC, Engstrom-Laurent A, Laurent UGB. Elimination of hyaluronic acid from the blood stream in the human. Clin Exp Pharmacol Physiol 1984;11:17–25.
[22] Fraser JRE, Laurent TC, Laurent UBG. Hyaluronan: its nature, distribution, functions and turnover. J Intern Med 1997;242:27–33.
[23] Oh EJ, Park K, Kim KS, Kim J, Yang JA, Kong JH, et al. Target specific and long-acting delivery of protein, peptide, and nucleotide therapeutics using hyaluronic acid derivatives. J Control Release 2010;141:2–12.
[24] Kim SJ, Hahn SK, Kim MJ, Kim DH, Lee YP. Development of a novel sustained release formulation of recombinant human growth hormone using sodium hyaluronate microparticles. J Control Release 2005;104:323–35.
[25] Jansen EJP, Emans PJ, Douw CM, Guldemond NA, Van Rhijn LW, Bulstra SK, et al. One intra-articular injection of hyaluronan prevents cell death and improves cell metabolism in a model of injured articular cartilage in the rabbit. J Orthop Res 2008;26:624–30.
[26] Maltese A, Borzacchiello A, Mayol L, Bucolo C, Maugeri F, Nicolais L, et al. Novel polysaccharides-based viscoelastic formulations for ophthalmic surgery: rheological characterization. Biomaterials 2006;27:5134–42.
[27] Yeom J, Bhang SH, Kim BS, Seo MS, Hwang EJ, Cho IH, et al. Effect of cross-linking reagents for hyaluronic acid hydrogel dermal fillers on tissue augmentation and regeneration. Bioconjug Chem 2010;21:240–7.
[28] Lapcik Jr L, Lapcik L, De Smedt S, Demeesters J, Chabrecek P. Hyaluronan: preparation, structure, properties, and applications. Chem Rev 1998;98:2663–84.
[29] Di Colo G, Zambito Y, Zaino C, Sanso M. Selected polysaccharides at comparison for their mucoadhesiveness and effect on precorneal residence of different drugs in the rabbit model. Drug Dev Ind Pharm 2009;35:941–9.
[30] Yenice I, Mocan MC, Palaska E, Bochot A, Bilensoy E, Vural I, et al. Hyaluronic acid coated poly-ϵ-caprolactone nanospheres deliver high concentrations of cyclosporine A into the cornea. Exp Eye Res 2008;87:162–7.
[31] De la Fuente M, Seijo B, Alonso MJ. Bioadhesive hyaluronan–chitosan nanoparticles can transport genes across the ocular mucosa and transfect ocular tissue. Gene Ther 2008;15:668–76.
[32] Moreira Jr CA, Armstrong DK, Jelliffe RW, Moreira AT, Woodford CC, Liggett PE, et al. Sodium hyaluronate as a carrier for intravitreal gentamicin. An experimental study. Acta Ophthalmol (Copenh.) 1991;69:45–9.
[33] Bae D, Gho Y, Yoon W, Chae C. Arginine-rich anti-vascular endothelial growth factor peptides inhibit tumor growth and metastasis by blocking angiogenesis. J Biol Chem 2000;275:13588–96.
[34] Monera OD, Sereda TJ, Zhou NE, Kay CM, Hodges RS. Relationship of sidechain hydrophobicity and alpha-helical propensity on the stability of the single-stranded amphipathic alpha-helix. J Pept Sci 1995;1:319–29.